

Chaperoning of Mutant p53 Protein by Wild-type p53 Protein Causes Hypoxic Tumor Regression*[§]

Received for publication, October 25, 2011, and in revised form, December 1, 2011. Published, JBC Papers in Press, December 6, 2011, DOI 10.1074/jbc.M111.317354

Rajan Gogna[‡], Esha Madan[‡], Periannan Kuppusamy[§], and Uttam Pati^{‡1}

From the [‡]Transcription and Human Biology Laboratory, School of Biotechnology, Jawaharlal Nehru University, New Delhi 110067, India and the [§]Davis Heart and Lung Research Institute, Department of Internal Medicine, Ohio State University, Columbus, Ohio 43210

Background: Hypoxia-induced p53 is transcriptionally inactive, and its molecular conformation and functional status in hypoxic tumors are unknown.

Results: WT p53 exists in mutant conformation in hypoxic tumors, and its conformation is oxygen-dependent. WT p53 functions as a molecular chaperone.

Conclusion: WT p53 chaperones and rescues mutant p53 in hypoxic tumors.

Significance: p53 chaperone therapy causes regression of hypoxic tumor xenografts through WT p53 chaperone activity.

Mutant (Mt) p53 abrogates tumor suppression functions of wild-type (WT) p53 through mutant-specific, gain-of-function effects, and patients bearing Mt p53 are chemoresistant. The dominant negative effect of p53 mutants results from their aggregation propensity which causes co-aggregation of WT p53. We explored the mechanism of p53 inactivation in hypoxia and hypothesized whether WT p53 could rescue Mt p53 in hypoxic tumors. WT p53 exists in mutant conformation in hypoxic core of MCF-7 solid tumors, and its conformation is oxygen-dependent. Under simulated hypoxia in cells, WT p53 undergoes conformational change in acquiring mutant conformation. An *in vivo* chaperone assay shows that WT p53 functions as a molecular chaperone in rescuing conformational and structural p53 mutants in cancer cells both at the transcription and proteome levels. WT p53 chaperone therapy is further shown to cause significant regression of tumor xenografts through reversion of the mutant phenotype to wild-type p53. The chaperone function of WT p53 is directly linked to the induction of apoptosis in both cancer cells and tumor xenografts. As oncogenic p53 mutants are linked to chemoresistance in hypoxic tumors, p53 chaperone therapy will introduce new dimensions to existing cancer therapeutics. We propose that in cancer cells, WT p53 chaperoning may either exist as a cellular event to potentially reverse the dominant negative effect of its oncogenic mutants or to stabilize yet unidentified factors.

Loss of the p53 gene or missense mutations that cause impairment of its transcriptional activity have been described in many tumors and are associated with inefficient DNA repair, genomic instability, reduced apoptosis, and, hence, increased oncogenicity. Hypoxia induces apoptosis *in vitro*; however, it fails to do so in solid tumors thus causing chemoresistance (1).

* This work was supported by grants from the Department of Biotechnology (India), and the University Grant Commission.

[§] This article contains supplemental Figs. S1–S8 and “Materials and Methods.”

¹ To whom correspondence should be addressed. Tel.: 919-312-401-811; E-mail: uttam@mail.jnu.ac.in.

In hypoxia, transcriptionally inactive p53 accumulates in both the cytoplasm and nucleus (2, 3) without the induction of its target genes (4–6), which could be due to post-transcriptional mechanism (3) or secondary effects such as acidosis caused by the hypoxic Pasteur effect (7); additional factors may also be involved (8). The introduction of WT p53 into tumor cells results in tumor regression (9–13) through enhancement of apoptosis (14) although the molecular mechanism of p53-induced effect is unknown. Structural p53 mutants are shown to inactivate the wild-type allele (15), and their dominant negative capacity and gain-of-function effect result from their aggregation propensity that causes co-aggregation of WT p53 (16).

In this study we have established a novel function of WT p53 that rescues mutant (Mt)² p53 in hypoxia. The inactivation of p53 in hypoxia is due its change in conformation which is oxygen-dependent. Introduction of WT p53 into a hypoxic tumor further causes regression of tumor thus suggesting that p53 chaperone therapy might be an integral part of cancer therapy protocol in the future.

MATERIALS AND METHODS

Cell Culture, Antibodies, and Transfections—MCF-7, HepG2, WRO, A-431, and DU-145 cells lines were obtained from National Center for Cell Sciences (Pune, India). H1299 cells with stable transfection of p53-CFP (p53-CFP H1299) were a gift from Neva Zatrovsky (Rehvtot). The cell lines were maintained in DMEM. Antibodies were p53C-ter anti-p53 pAb421 (nonconformational), anti-p53 pAb1620 (WT conformation), and anti-p53 pAb240 (Mt conformation) (Calbiochem). All transfections were carried out using Effectene transfection reagent (Qiagen) according to the manufacturer's instructions.

Electron Paramagnetic Resonance (EPR) Oximetry—Lithium octa-*n*-butoxy 2,3-naphthalocyanine microcrystals were used for tissue oxygen measurements. Ten-microgram microcrystals were resuspended in 500 μ l of DMEM. Twenty-five micro-

² The abbreviations used are: Mt, mutant; CT, core tissue; IP, immunoprecipitation; NTD, N-terminal domain; PT, peripheral tissue.

Wild-type p53 Rescues Mutant p53

liters of this suspension were added to 5×10^5 cells for each 100- μ l injection. Oxygen measurements were performed immediately, weekly, and upon sacrifice using *in vivo* EPR oximetry. Measurements of tumor oxygenation were performed using an L-band *in vivo* EPR spectrometer (L-band; Magnetech). Mice were placed in a right, lateral position with their tumor close to the surface coil resonator. EPR spectra were acquired as single 30-s scans. The instrument settings were as follows: incident microwave power, 4 mW; modulation amplitude, 180 mG; modulation frequency, 100 kHz; receiver time constant, 0.2 s. The peak-to-peak width of the EPR spectrum was used to calculate pO_2 using a standard calibration curve.

Live Cell Imaging—For live cell imaging, p53-CFP H1299 cells were plated on a glass-bottom dish with a coverslip (MatTek). The dish was placed either on an inverted microscope (Ti-E; Nikon) or on a confocal microscope (FV-1000; Olympus). Both microscopes featured a culture system (Tokai Hit) at 37 °C under 5% CO₂, and 1.8% hypoxia was maintained using Ibidi gas incubation systems (GmbH, Germany). Wide field fluorescence images were captured using a Ti-E under the operation of NIS Elements version 3.0 (Nikon) with a PlanApo VC $\times 100$ (NA = 1.4) oil-immersion objective lens equipped with an electron multiplying charge-coupled device (iXon+; Andor; normal mode; gain $\times 5.1$) with filter sets for CFP; the exposure period was set to 100–1000 ms. A 75-W xenon lamp was used as a light source. Fluorescence intensity was measured using Metamorph version 7.5 (Molecular Devices) and plotted using Origin version 7 (OriginLab).

MRI Analysis—The imaging was performed using a Bruker Biospin 94/30 magnet (Bruker Biospin, Karlsruhe Germany). The animals were anesthetized with 2% isoflurane mixed with 1 liter/min carbogen (95% oxygen/5% carbon dioxide mixture). Anesthesia was maintained using 1–1.5% isoflurane. Respiration measurements were monitored during image acquisition using a small animal monitoring system (model 1025, Small Animal Instruments, Inc.; Stony Brook, NY). Body temperature was monitored using a rectal thermometer and maintained using water-heated bedding. Anatomic images were collected with following parameters: TR = 1200 ms, TE = 7.5 ms, TE = 12 ms, rare factor = 4, navgs = 4 for T1-weighted images; TR = 3500 ms, TE = 36 ms, rare factor = 8, navgs = 4, for T2-weighted. The acquisition parameters for both the T1- and T2-weighted multislice scans were as follows: FOV = 20 mm \times 20 mm, slice thickness = 1.0 mm, matrix size = 256 \times 256 pixels.

For additional procedures, see supplemental Materials and Methods.

RESULTS

WT p53 Exists as Mutant Conformation in Hypoxic Tumors—The oxygen concentration varies in solid tumors, and the conformational status of p53 under low oxygen density in the core of solid tumors is unknown. To probe whether the p53 conformation is oxygen-dependent we first determined the oxygen tension in MCF-7 tumor (p53^{+/+}) xenografts (>1.4 cm³) by noninvasive (spectral-spatial) *in vivo* EPR oximetry three-dimensional imaging (Fig. 1a). Using lithium octa-*n*-butoxy 2,3-naphthalocyanine as the probe (17), oxygen measurements

were performed weekly. Measurements of tumor oxygenation were performed using an L-band *in vivo* EPR spectrometer (L-band). EPR spectra were acquired as single 30-s scans. The value of the pO_2 in the tissue was found to be 1.8% from a standard curve of the EPR line width *versus* the oxygen concentration; the mean oxygen concentration levels of 1.3% are common in vascular tumors and are considered hypoxic (18). In hypoxic tumor core tissue (CT) the level of p53 protein was 6-fold (Fig. 1b), and RNA was 10-fold (supplemental Fig. S1) higher, respectively, when it was compared with peripheral tissue (PT). p53 was exclusively present as a conformational mutant in the CT, and the level of WT p53 was very low. The p53 conformation was analyzed by immunoprecipitation (IP) using p53 conformational antibodies (pAb1620, WT; pAb240, Mt) (Fig. 1b). The total p53 was detected by p53-Cter antibody pAb421. The function of p53 correlates with its WT conformation, specifically recognized by antibodies pAb1620, and many cancer-associated mutations cause loss of this conformation thus failing to bind denatured p53 (19). pAb1620 recognizes residues Arg¹⁵⁶, Leu²⁰⁶, Arg²⁰⁹, and Gln/Asn²¹⁰. pAb240 defines a novel, highly conserved, denaturation-resistant epitope on p53; it binds to p53 in the Mt conformation and also to denatured p53. Different p53 mutants react more strongly with pAb240 than with pAb1620 (20). Both antibody epitopes are far from the p53 interface with DNA, but near the epitope of the Mt conformation antibody pAb240. The results suggest that the observed conformation change in hypoxic core may be linked to low oxygen.

p53 Conformation Is Oxygen-dependent—To validate this finding in cells, p53-CFP H1299 stable cells were subjected to physiological hypoxia (1.8% O₂, 0–72 h), and p53 conformation was analyzed by *in vivo* ELISA. In early hypoxia (6–12 h), p53 (1620) WT conformation was at the highest, and at 72 h it was at the lowest level (Mt:WT, 5:1) which suggests that p53 conformation is linked to cellular oxygen concentration (Fig. 1c). The decrease in Mt (240) conformation and rise in WT (1620) conformation at 12 h may be due to stabilization of p53 in early hypoxia. It is established that in early hypoxic shock WT p53 gets stabilized (3, 21). However, the combined level of 1620 and 240 forms remains same all the time, similar to that of total p53 level at 0 h under normoxia (Fig. 1c). After 12 h, as the cell perceives the hypoxic stress to be continuous, WT p53 then gradually switches to Mt p53 over 72 h. To further reaffirm this finding, in parallel, we utilized stable p53-CFP H1299 cells and monitored the p53 conformation through measuring the CFP fluorescence intensity both by flow cytometry and live cell imaging (Fig. 1, e and f). We rationalized that CFP fluorescence might change (Fig. 1d) if WT p53 undergoes conformational change, probably, in the DNA-binding domain under low oxygen (22). Approximately 95% of the malignant mutations occur in the p53 DNA-binding domain thus causing p53 conformational change; invariably, a conserved aggregation nucleating sequence within this domain was shown to be responsible for mutant p53 aggregation (16). For live cell imaging, a confocal microscope (FV-1000; Olympus) featured with a culture system (Tokai Hit) at 37 °C under 5% CO₂ and 1.8% hypoxia was maintained using Ibidi gas incubation systems. Fluorescence intensity was measured using Metamorph version 7.5 and plotted

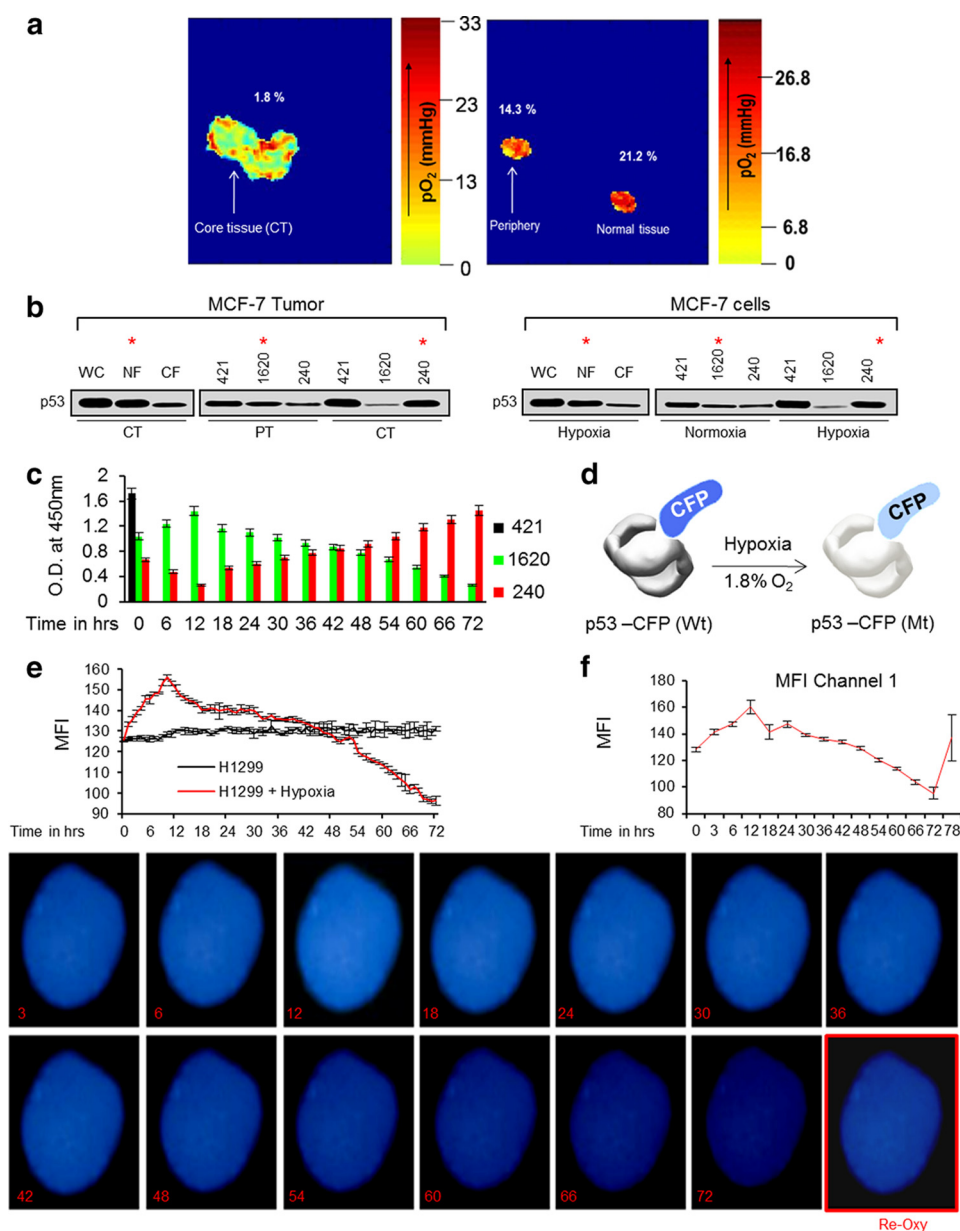


FIGURE 1. p53 conformation is dependent upon oxygen concentration. *a*, oxygen concentration in the core and peripheral regions of MCF-7 tumors (14 day, 2 cm³) was analyzed using EPR oxymetry. Core tissue (CT) and peripheral tissue (PT) have 1.8% and 14.3% O₂, respectively (*n* = 5). *b*, left, in MCF-7 tumors CT and PT were excised; CT was separated into whole cell (WC), nuclear fraction (NF) and cytoplasmic fraction (CF) to study p53 level. IP showed high p53 level in NF of CT (second lane). p53 conformation was analyzed with p53 conformational antibodies pAb1620 (WT) and pAb240 (Mt); in PT, p53 was in 1620 (fifth lane), and in CT it was exclusively in 240 conformation (seventh lane). *b*, right, hypoxic (1.8% O₂) MCF-7 cells were divided into WC, NF, and CF; p53 was in high level in NF (second lane) and in 240 conformation (ninth lane). *c*, *in vivo* ELISA of hypoxic p53-CFP H1299 cells shows that p53 undergoes conformational change from 1620 to 240 conformation (0–72 h). 1620 conformation was stabilized in early hypoxia (6–12 h) and then decreased with increasing hypoxia exposure; total p53 (black), 1620 (green), and 240 (red) (*n* = 11, S.D. (error bars), ANOVA). *d*, model depicts hypothesis that CFP-p53 may undergo conformational change in hypoxia. *e*, fluorescence intensity of p53-CFP H1299 cells was analyzed under normoxia (black) and hypoxia (red) using flow cytometry; stable p53-CFP fluorescence is shown in normoxic cells, with a rise in early hypoxia followed by a decrease in fluorescence (48–72 h). *f*, live cell imaging of p53-CFP H1299 cells shows that fluorescence increased between 6 and 12 h (compare *c* and *d*) and then gradually decreased over 72 h (refer to MFI plot) (*n* = 15, S.D., ANOVA). Reoxygenation induced a sharp increase in p53-CFP fluorescence (last image) (*n* = 15), suggesting O₂-dependent conformational change in p53.

using Origin version 7. Both flow cytometry and live cell imaging analysis show that the fluorescence intensity of the p53-CFP chimeric protein first increases at 12–18 h (Fig. 1, *e* and *f*), which may probably be due to early hypoxic shock (compare this with rise of the 1620 conformation, Fig. 1*c*), followed by the gradual decrease in fluorescence intensity up to >90% at the end of 72 h (Fig. 1*f*). Interestingly, in live cell imaging, reoxygenation at 72 h restores the fluorescence (78 h), which suggests that p53 conformation is reversibly oxygen-dependent.

WT p53 Functions as a Molecular Chaperone—Molecular chaperones have been shown to remodel the conformation of activators in controlling rapid reversible transcriptional response (23) and are known to enhance both p53-mediated trans-activation. They were shown to influence hormone receptor activity differentially; a GAL4-p23 construct had 35-fold inhibitory effect on GR-dependent activity and 100-fold inhibitory effect on TR-dependent activity (24). CHIP (25), HSP90, and HSP70 (26) support p53 tumor suppressor func-

Wild-type p53 Rescues Mutant p53

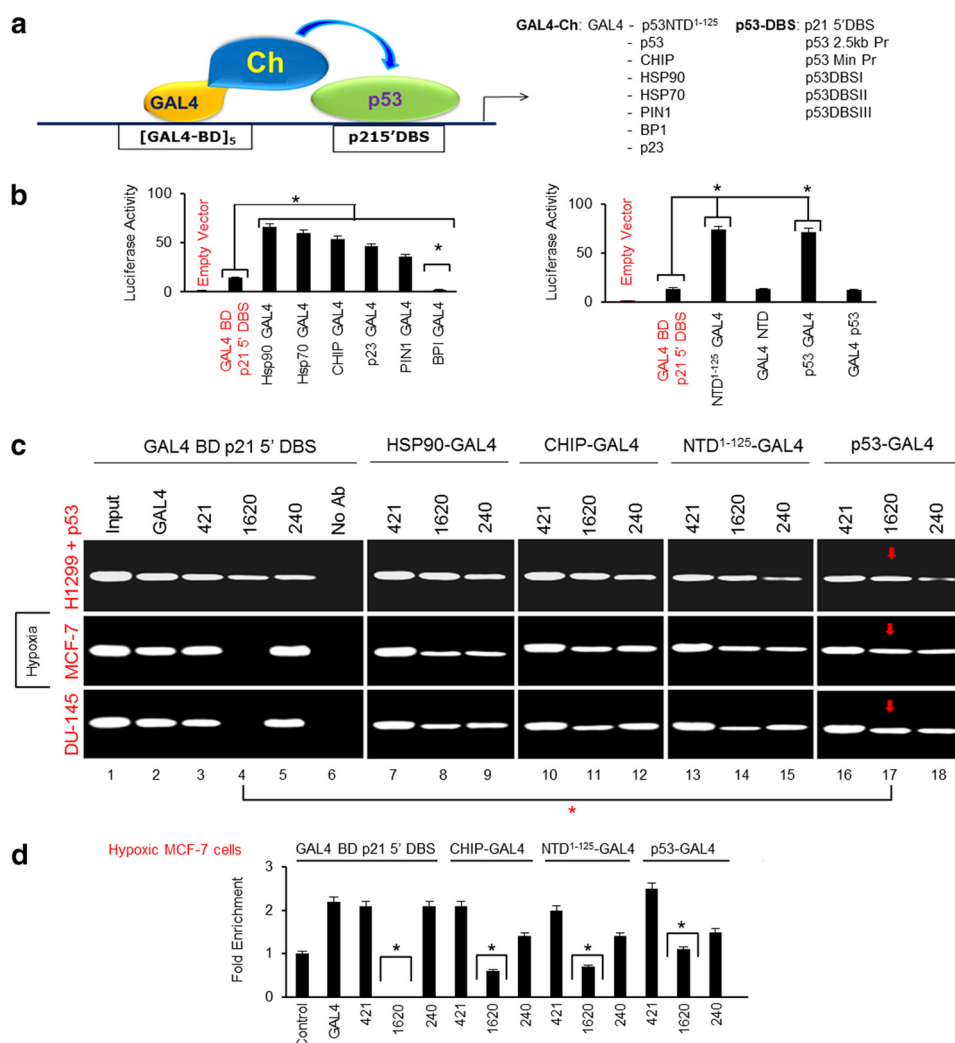


FIGURE 2. WT p53 functions as a molecular chaperone. *a*, model explains the design for *in vivo* chaperone assay, which shows various GAL4-Ch and p53-DBS-luciferase constructs (*right b*), in the luciferase assay, GAL4BD-p21 5'-p53-DBS was co-transfected with WT p53 cDNA and GAL4(NTD¹⁻¹²⁵), p53, HSP90, HSP70, CHIP, p23, PIN1, BP1 constructs in H1299 cells and luciferase activity was measured, in H1299 cells. The luciferase activity induced by GAL4BD-p21 5'-p53-DBS and p53 cDNA (*right*) (second lane) was taken as base line. In control, HSP90, HSP70, CHIP, p23, and PIN1 were able to chaperone p53 bound to the p21 5' site and increase the luciferase activity (p53 inhibitor BP1; negative control). GAL4BD-p21 5'-p53-DBS was then co-transfected with p53-GAL4 or NTD¹⁻¹²⁵-GAL4 (free NTD) or with GAL4-p53 or GAL4-NTD¹⁻¹²⁵ (NTD constrained); results show that NTD¹⁻¹²⁵-GAL4 (*second lane*) and p53-GAL4 (*fifth lane*) chaperoned p53 anchored upon p21 5'-p53-DBS, whereas GAL4-NTD¹⁻¹²⁵ (*fourth lane*) and GAL4-p53 (*sixth lane*) failed ($n = 10$, S.D. (error bars), ANOVA). Chaperone activity of p53-GAL4 was higher than HSP90. *c*, ChIP was performed on the GAL4-p21 5'-p53-DBS luciferase vector using pAb421 (p53-Cter), pAb1620 (WT), and pAb240 (Mt) in H1299 (+WT-p53 cDNA), hypoxic MCF-7, and DU-145 cells. ChIP shows that both mutant and wild-type p53 were present in equal ratio on p21 5'-p53-DBS in H1299 cells (+wt-p53 cDNA) (*top row, lanes 4 and 5*); in hypoxic MCF-7 and normoxic DU-145 cells (*Input, GAL4 Ab ChIP; positive controls*) p53 exclusively present in mutant (240) conformation (*lane 5*). Addition of HSP90-GAL4, CHIP-GAL4, NTD¹⁻¹²⁵-GAL4, and p53-GAL4 increased p53-1620 conformation considerably upon promoter (*lanes 8, 11, 14, and 17*). *d*, results were repeated using real-time ChIP ($n = 8$, S.D., ANOVA).

tion under stress conditions. As intrinsically disordered p53 N-terminal domain (NTD¹⁻¹²⁵) stabilizes WT p53 under stress we earlier had proposed that it might possess a self-chaperoning role as an uncleaved molecule (27). To prove this hypothesis, we first performed an *in vivo* GAL4-chaperone assay in H1299 (p53^{-/-}) cells (Fig. 2*a* and supplemental Figs. S2 and S3) utilizing p53 cDNA and GAL4BD-p21 5'-DBS-luciferase constructs (p21 5'DBS). The above constructs were transiently co-transfected with p53-GAL4 or NTD¹⁻¹²⁵-GAL4 cDNA. Both chimeric constructs increase luciferase activity by 6-fold when NTD¹⁻¹²⁵ domain is kept free (Fig. 2*b, right, fifth and third lanes*), suggesting that WT p53 possesses autochaperone activity that is responsible for enhancing DNA binding conformation of p53. However, the chaperone activities of both NTD¹⁻¹²⁵ and

p53 were equally suppressed when the NTD¹⁻¹²⁵ domain was restrained (Fig. 2*b, right, sixth and fourth lanes*) which suggests that the chaperone function of p53 is linked to its intrinsically disordered character. Surprisingly, the chaperone activity of WT p53 or NTD¹⁻¹²⁵ is higher than HSP90 and CHIP, two known chaperones for WT p53 (Fig. 2*b, left, third and fifth lanes*). In a control experiment, the chaperone activity of various GAL4 chaperones is shown to be in the following order: HSP90 > HSP70 > CHIP > p23 > PIN1 > BP1 (Fig. 2*b*). To check whether WT p53 chaperoning results in activation of p53 promoter we utilized chimeric constructs of p53 minimal promoter (+1 to -419), or its DBS I, II, and III, fused to GAL4BD, and subjected them to co-transfection with NTD¹⁻¹²⁵-GAL4 or p53-GAL4 cDNA (supplemental Fig. S4).

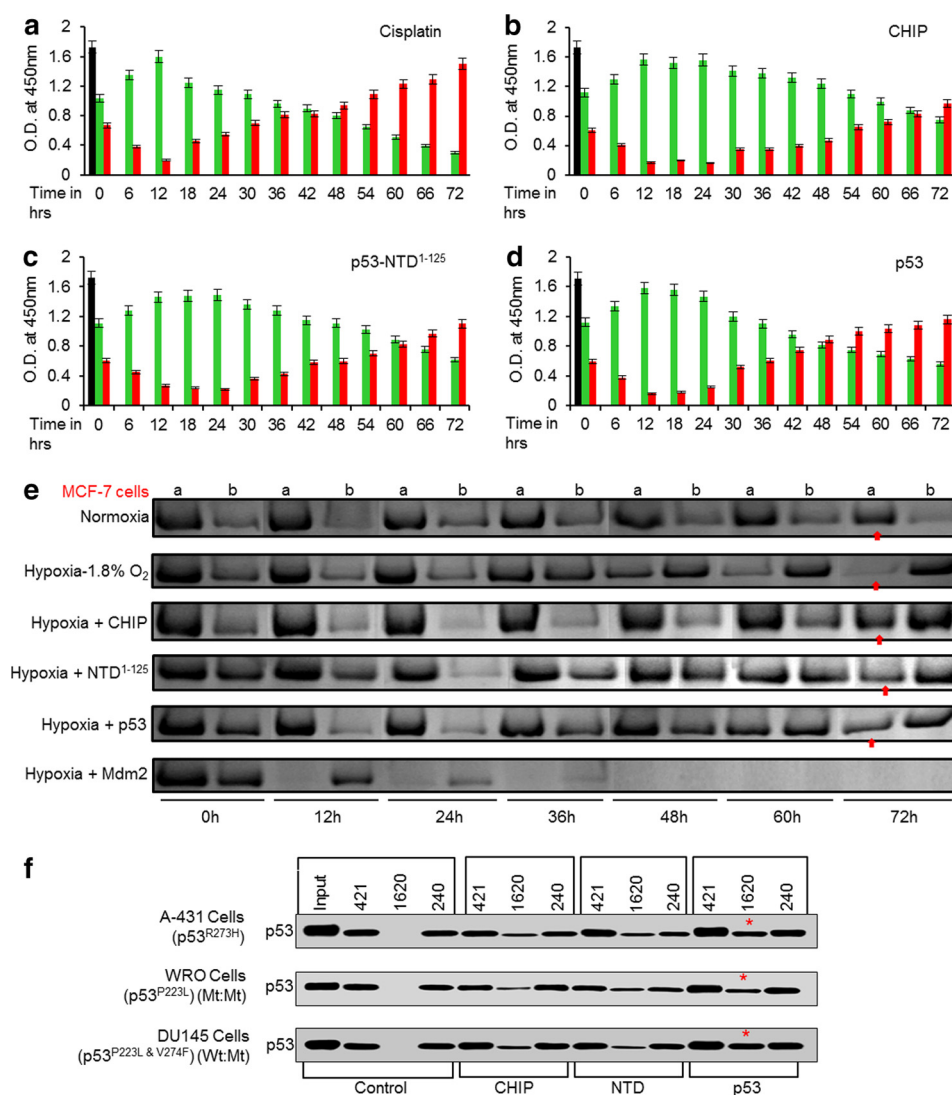


FIGURE 3. WT p53 rescues both conformational and structural Mt p53. *a*, *in vivo* ELISA of hypoxic p53-CFP H1299 cells was conducted to observe p53 conformation shift upon addition of p53, NTD¹⁻¹²⁵, and CHIP; pAb421 (p53-C-ter) (black), pAb1620 (WT) (green) and pAb240 (Mt) (red). Cisplatin failed to induce change in p53 conformation. *b–d*, p53, NTD¹⁻¹²⁵, and CHIP increased the 1620 conformation by 2–2.50 ($n = 11$, S.D. (error bars), ANOVA). *e*, IP with pAb1620 (*a*) and pAb240 (*b*) of MCF-7 cells shows that 1620 level is maintained. In hypoxic MCF7 cells (0–72 h), 1620 level declined and was absent at 72 h; only 240 form was present. Addition of CHIP, NTD¹⁻¹²⁵, and p53 increases 1620 conformation (black arrow) under hypoxia (Mdm2 negative control) ($n = 8$). *f*, IP of normoxic A-431 (p53^{R273H}), mutant cancer cell line), DU-145 (heterozygous, p53WT/Mt (p53^{P223L/V274F}), and WRO (homozygous, Mt/Mt) cells with pAb1620 and pAb240 show absence of 1620. Addition of CHIP, NTD¹⁻¹²⁵, and WT p53 cDNA (5 μ g of DNA) induced conversion of 240 form to 1620 form conformation both in WRO and DU-145 cells ($n = 8$).

The promoter activity of the p53 minimal promoter is comparable with the 2.5-kb full-length promoter (supplemental Fig. S5, *second* and *fourth* lanes). Both NTD¹⁻¹²⁵-GAL4 and p53-GAL4 increased luciferase activity by 2-fold (supplemental Fig. S5, *seventh* and *eighth* lanes) via selective activation of p53 by WT p53 upon DBS II (supplemental Fig. S5, *14th* and *15th* lanes), thus confirming p53 autochaperoning.

To exclude the possibility that p53-GAL4 does not compete with p53 in selecting p21 5'-DBS, competitive chromatin immunoprecipitation assay (ChIP) was conducted; as was expected, p53-GAL4 preferentially selects GAL4-BD site and not vice versa upon p53 promoter (supplemental Fig. S6). To analyze whether autochaperoning occurs after p53-GAL4 or NTD¹⁻¹²⁵-GAL4 anchor upon GAL4-BDp21 5'-DBS (supplemental Fig. S2), in enhancing DNA-binding conformation of p53 (1620), a transient ChIP assay (28) was done utilizing pAb1620 and pAb240, in H1299 (p53^{-/-}), hypoxic MCF-7

(p53^{+/+}), and normoxic DU-145 (p53WT/Mt) cells. In control H1299 cells, the transfection of p53 cDNA shows that the ratio of WT to Mt (1620:240) upon p21 5'-DBS is 1:1 (Fig. 2c, *top row*, lanes 4 and 5); transfection of p53-GAL4 or NTD¹⁻¹²⁵-GAL4 resulted in increase in wild-type (Fig. 2c, *top row*, lanes 11 and 14) and decrease in mutant conformation upon p21 5'-DBS (Fig. 2c, *top row*, lanes 12 and 15). However, in hypoxic MCF-7 and normoxic DU-145 cells, p53 upon p21 5'-DBS was exclusively present in the mutant conformation (240) (Fig. 2c, *middle* and *bottom* rows, lane 4). p53-GAL4 and NTD¹⁻¹²⁵-GAL4 rescue Mt p53 and stabilized WT p53 (Fig. 2c, *middle* and *bottom* rows, lanes 11 and 14) significantly upon p21 5'-DBS, establishing that p53 rescues mutant p53 at the transcription level. HSP90-GAL4 and CHIP-GAL4 are used as controls and they both rescue p53 mutants (Fig. 2c). Real-time transient ChIP analysis (Fig. 2d and supplemental Fig. S7) confirms that in hypoxic MCF-7 and normoxic DU-145 cells mutant p53 is rescued by wild-type p53.

Wild-type p53 Rescues Mutant p53

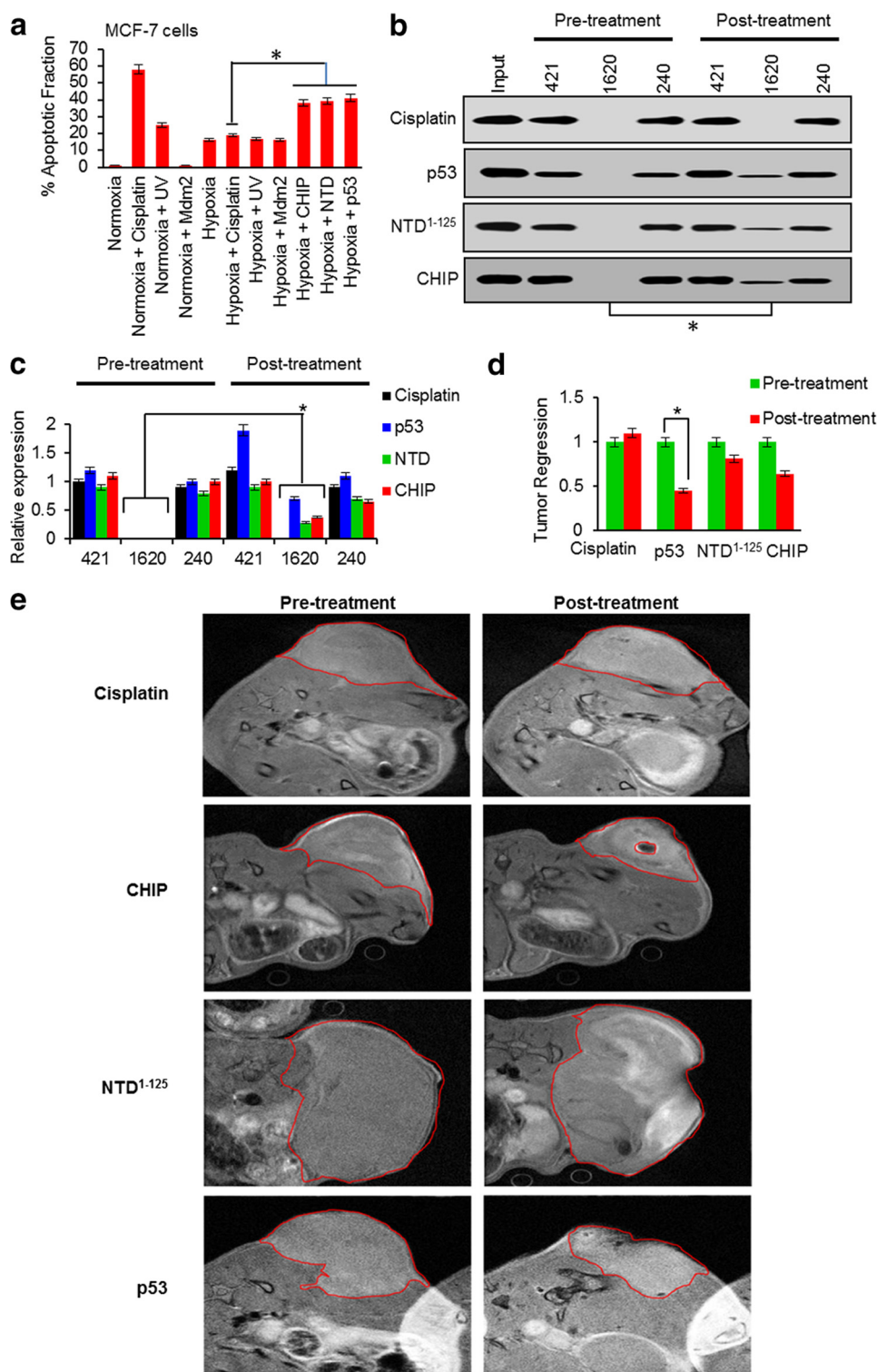


FIGURE 4. WT-p53 rescues Mt-p53 and causes regression of hypoxic tumor. *a*, apoptosis was measured in MCF-7 cells in hypoxic condition in presence of cisplatin, UV, CHIP, NTD¹⁻¹²⁵, and p53. Cisplatin and UV did not induce apoptosis in hypoxic MCF-7 cells (sixth lane); p53 chaperoning by CHIP, NTD¹⁻¹²⁵, and WT p53 caused induction of apoptosis >2.5-fold compared with hypoxia ($n = 10$) (S.D. (error bars), ANOVA). *b*, MCF-7 tumors (2 cm³) were treated with molecular chaperones (CHIP, NTD¹⁻¹²⁵, and WT p53) ($n = 7$, each group). Core tissue of control and treated mice were excised to study p53 conformational status. In pretreatment tumors, p53 exclusively exists in 240 conformation. Cisplatin has no effect upon p53 conformation. WT p53, NTD¹⁻¹²⁵, and CHIP induced a significant increase in 1620 conformation. *c*, *in vivo* ELISA was conducted to validate IP result. *d* and *e*, MCF-7 tumors were treated with cisplatin and molecular chaperones (CHIP, NTD¹⁻¹²⁵, and WT p53), and MRI was conducted to study tumor volume in pre- and post-treatment (48 h) groups. Cisplatin did not affect the tumor volume whereas transfection of p53 resulted in regression of tumor (64%); CHIP and NTD¹⁻¹²⁵ showed regression by 37 and 29%, respectively.

WT p53 Rescues Mt p53 in Cancer Cells—To establish whether WT p53 can rescue conformational Mt p53, MCF-7 cells were subjected to hypoxia, and p53 conformation was ana-

lyzed by *in vivo* ELISA. Both p53 and NTD¹⁻¹²⁵ rescued Mt p53, thus stabilizing WT p53 by >2-fold (Fig. 3, *c* and *d*) whereas cisplatin fails to rescue Mt p53 (Fig. 3*a*, compare Fig. 1*c*). Fur-

ther, IP utilizing conformational antibodies pAb1620 and pAb240 shows that WT p53 and NTD¹⁻¹²⁵ rescued Mt p53 at 72 h of hypoxic exposure (Fig. 3e). The level of WT p53 (1620) started declining gradually (compare with Fig. 1c) and was not detected at 72 h. Transfection of p53 or NTD¹⁻¹²⁵ cDNA resulted in restoration of WT p53 (1620); its level was comparable with normoxic cells. To check whether p53 and NTD¹⁻¹²⁵ can rescue structural p53 mutants, A-431 (p53^{R273H}) (29), WRO (p53 WT/Mt), and DU145 (p53 Mt/Mt) cells were selected in which p53 is present as mutants (Fig. 3f). WRO is a homozygous, p53 Mt cell line (30) that has a mutation at codon 223 (p53^{P223L}). However, DU145 is a heterozygous human prostate carcinoma cell line that harbors a temperature-sensitive allele of p53 (p53^{P223L/V274F}) (31). Transfection of p53 cDNA resulted in rescue of Mt p53 in these cell types. The level of p53 (1620) (after transfection with p53 cDNA) was higher when it was compared with the transfection result of NTD¹⁻¹²⁵ and CHIP cDNA which could be due to the exogenous p53 expression level. The dominant negative inactivation of WT p53 results from tetramerization that is caused by mixed incorporation of wild-type and mutant DNA-binding domains into a single tetramer (32, 33) and due to nucleation that is greatly enhanced by the tetramerization domain. We suggest that in a role reversal model, the observed rescue of Mt p53 by p53 chaperoning is interesting and it may well be a “reverse” nucleation process (16) due to intermolecular interaction of NTD¹⁻¹²⁵ with the tetramerization domain (16).

p53 Chaperone Therapy Causes Regression of Hypoxic Tumors—As small molecules are shown to restore Mt p53 in to WT p53 in triggering apoptosis (14, 34, 35), we then measured p53- or NTD¹⁻¹²⁵-mediated cellular apoptosis in hypoxic MCF-7 cells by annexin-V staining; p53- and NTD¹⁻¹²⁵-treated cells increased apoptosis by >2.5-fold (Fig. 4a). The expression of the p53 downstream genes was then analyzed in hypoxic MCF-7 cells transfected with p53cDNA (supplemental Fig. S8). The real-time PCR analysis shows significant increase in the expression of 88 p53 downstream genes involved in p53 signaling in hypoxic MCF-7 cells. The therapeutic potential of this finding was further realized by inducing p53-mediated MCF-7 tumor regression in mice followed by analysis with MRI (Fig. 4a). In MCF-7 tumor xenografts, p53/NTD¹⁻¹²⁵/CHIP cDNA were transfected in to the core region of MCF-7 tumors through PEG liposome-based *in vivo* transfection reagent (Altogen Biosystems), and the MRI was performed using a Bruker Biospin 94/30 magnet (Bruker Biospin). Anatomic images were collected with following parameters: TR = 1200 ms, TE = 7.5 ms, TE = 12 ms, rare factor = 4, navgs = 4 for T1-weighted images; TR = 3500 ms, TE = 36 ms, rare factor = 8, navgs = 4, for T2-weighted. The acquisition parameters for both the T1- and T2-weighted multislice scans were as follows: FOV = 20 mm x 20 mm, slice thickness = 1.0 mm, matrix size = 256 × 256 pixels. *In vivo* transfection of p53 or NTD¹⁻¹²⁵ cDNA in to the core of MCF-7 tumors results in significant reduction in tumor volume at 48 h by 64 and 29%, respectively (Fig. 4, d and e); CHIP, a known chaperone of p53, reduced tumor volume by 37%. Further, in an excised tumor, p53 is present exclusively in mutant conformation (Fig. 4, b and c);

convincingly, a post-treatment excised tumor shows effective restoration of pAb1620 conformation (Fig. 4, b and c).

DISCUSSION

A number of clinical trials have been shown to restore expression of wild-type p53 in tumor cells in patients with varieties of advanced cancer including Li-Fraumeni syndrome embryonal carcinoma with adenoviral vectors, in the absence of significant toxicity (10, 11). Although research on mutant p53 is entering the clinical and translational era, the detailed functions of p53 in normal cells, and even more so in cancer cells, remain obscure (30, 31). In a role reversal, the new function of WT p53 as a molecular chaperone in rescuing its mutant in hypoxic tumors thus explains the molecular mechanism of p53-dependent apoptosis and tumor regression. Our data thus establish that wild-type p53-mediated tumor regression is conclusively linked to the role of WT p53 as a molecular chaperone which will introduce a new dimension to the existing array of cancer therapeutics. Although the chaperone (Fig. 2b) and apoptotic potential of WT p53 (Fig. 4a) are comparable with those of NTD¹⁻¹²⁵, the tumor regression potential of NTD¹⁻¹²⁵ (Fig. 4, d and e) is about half of WT p53, which suggests that additional *in vivo* p53-bound modulating factors may also be involved in tumor regression. The NTD might also bind to the p53 C-terminal domain in inhibiting p53 function (36). Because both structural and conformational p53 mutants are linked to chemoresistance in varieties of tumors, p53 chaperone therapy will introduce a new dimension to the existing array of cancer therapeutics. The novel role of WT p53 as a molecular chaperone in rescuing its mutants in hypoxia and in regression of hypoxic tumor raises a question of whether p53 self-rescue may exist as a cellular event to reverse the oncogenic activities of Mt p53 in cancer cell; the self-rescue mode may exist as a natural but simultaneous phenomenon in cell that could be linked to the response of the cell to the environment. Future strategy will address whether p53 chaperoning of yet other unidentified substrates may be involved in cancer progression.

Acknowledgments—We thank N. Zatrovsky for the p53-CFP H1299 cell line; C. De-Primo for live cell imaging; T. Kouzarides for the GAL4-DBD construct; L. Citro for MRI; B. Lalhal, N. Bishnoi, P. Kumar, and R. Ranjan for GAL4-chaperone constructs, and K. Gupta for assistance. A. Bratasz and L. Citro for the EPR and MRI measurements.

REFERENCES

- Schnitzer, S. E., Schmid, T., Zhou, J., and Brüne, B. (2006) Hypoxia and HIF-1 α protect A549 cells from drug-induced apoptosis. *Cell Death Differ.* **13**, 1611–1613
- Ashcroft, M., Taya, Y., and Vousden, K. H. (2000) Stress signals utilize multiple pathways to stabilize p53. *Mol. Cell. Biol.* **20**, 3224–3233
- Koumenis, C., Alarcon, R., Hammond, E., Sutphin, P., Hoffman, W., Murphy, M., Derr, J., Taya, Y., Lowe, S. W., Kastan, M., and Giaccia, A. (2001) Regulation of p53 by hypoxia: dissociation of transcriptional repression and apoptosis from p53-dependent transactivation. *Mol. Cell. Biol.* **21**, 1297–1310
- Achison, M., and Hupp, T. R. (2003) Hypoxia attenuates the p53 response to cellular damage. *Oncogene* **22**, 3431–3440
- Hammond, E. M., and Giaccia, A. J. (2006) Hypoxia-inducible factor-1 and

- p53: friends, acquaintances, or strangers? *Clin. Cancer Res.* **12**, 5007–5009
6. Liu, T., Laurell, C., Selivanova, G., Lundberg, J., Nilsson, P., and Wiman, K. G. (2007) Hypoxia induces p53-dependent transactivation and Fas/CD95-dependent apoptosis. *Cell Death Differ.* **14**, 411–421
 7. Pan, Y., Oprysko, P. R., Asham, A. M., Koch, C. J., and Simon, M. C. (2004) p53 cannot be induced by hypoxia alone but responds to the hypoxic microenvironment. *Oncogene* **23**, 4975–4983
 8. Bourdon, J. C., Khoury, M. P., Diot, A., Baker, L., Fernandes, K., Aoubala, M., Quinlan, P., Purdie, C. A., Jordan, L. B., Prats, A. C., Lane, D. P., and Thompson, A. M. (2011) p53 mutant breast cancer patients expressing p53 γ have as good a prognosis as wild-type p53 breast cancer patients. *Breast Cancer Res.* **13**, R7
 9. Martins, C. P., Brown-Swigart, L., and Evan, G. I. (2006) Modeling the therapeutic efficacy of p53 restoration in tumors. *Cell* **127**, 1323–1334
 10. Sauter, E. R., Takemoto, R., Litwin, S., and Herlyn, M. (2002) p53 alone or in combination with antisense cyclin D1 induces apoptosis and reduces tumor size in human melanoma. *Cancer Gene Ther.* **9**, 807–812
 11. Senzer, N., Nemunaitis, J., Nemunaitis, M., Lamont, J., Gore, M., Gabra, H., Eeles, R., Sodha, N., Lynch, F. J., Zumstein, L. A., Menander, K. B., Sobol, R. E., and Chada, S. (2007) p53 therapy in a patient with Li-Fraumeni syndrome. *Mol. Cancer Ther.* **6**, 1478–1482
 12. Ventura, A., Kirsch, D. G., McLaughlin, M. E., Tuveson, D. A., Grimm, J., Lintault, L., Newman, J., Reczek, E. E., Weissleder, R., and Jacks, T. (2007) Restoration of p53 function leads to tumour regression *in vivo*. *Nature* **445**, 661–665
 13. Xue, W., Zender, L., Miething, C., Dickins, R. A., Hernando, E., Krizhanovsky, V., Cordon-Cardo, C., and Lowe, S. W. (2007) Senescence and tumour clearance is triggered by p53 restoration in murine liver carcinomas. *Nature* **445**, 656–660
 14. Vazquez, A., Bond, E. E., Levine, A. J., and Bond, G. L. (2008) The genetics of the p53 pathway, apoptosis and cancer therapy. *Nat. Rev. Drug Discov.* **7**, 979–987
 15. Milner, J., and Medcalf, E. A. (1991) Cotranslation of activated mutant p53 with wild type drives the wild-type p53 protein into the mutant conformation. *Cell* **65**, 765–774
 16. Xu, J., Reumers, J., Couceiro, J. R., De Smet, F., Gallardo, R., Rudyak, S., Cornelis, A., Rozenski, J., Zwolinska, A., Marine, J. C., Lambrechts, D., Suh, Y. A., Rousseau, F., and Schymkowitz, J. (2011) Gain of function of mutant p53 by coaggregation with multiple tumor suppressors. *Nat. Chem. Biol.* **7**, 285–295
 17. Kuppusamy, P., Li, H., Ilangovan, G., Cardounel, A. J., Zweier, J. L., Yamada, K., Krishna, M. C., and Mitchell, J. B. (2002) Noninvasive imaging of tumor redox status and its modification by tissue glutathione levels. *Cancer Res.* **62**, 307–312
 18. Vaupel, P., Höckel, M., and Mayer, A. (2007) Detection and characterization of tumor hypoxia using pO₂ histography. *Antioxid. Redox Signal.* **9**, 1221–1235
 19. Wang, P. L., Sait, F., and Winter, G. (2001) The “wild-type” conformation of p53: epitope mapping using hybrid proteins. *Oncogene* **20**, 2318–2324
 20. Gannon, J. V., Greaves, R., Iggo, R., and Lane, D. P. (1990) Activating mutations in p53 produce a common conformational effect: a monoclonal antibody specific for the mutant form. *EMBO J.* **9**, 1595–1602
 21. Graeber, T. G., Peterson, J. F., Tsai, M., Monica, K., Fornace, A. J., Jr., and Giaccia, A. J. (1994) Hypoxia induces accumulation of p53 protein, but activation of a G₁ phase checkpoint by low-oxygen conditions is independent of p53 status. *Mol. Cell. Biol.* **14**, 6264–6277
 22. Waldo, G. S., Standish, B. M., Berendzen, J., and Terwilliger, T. C. (1999) Rapid protein-folding assay using green fluorescent protein. *Nat. Biotechnol.* **17**, 691–695
 23. Nollen, E. A., and Morimoto, R. I. (2002) Chaperoning signaling pathways: molecular chaperones as stress-sensing “heat shock” proteins. *J. Cell Sci.* **115**, 2809–2816
 24. Freeman, B. C., and Yamamoto, K. R. (2002) Disassembly of transcriptional regulatory complexes by molecular chaperones. *Science* **296**, 2232–2235
 25. Tripathi, V., Ali, A., Bhat, R., and Pati, U. (2007) CHIP chaperones wild-type p53 tumor suppressor protein. *J. Biol. Chem.* **282**, 28441–28454
 26. Walerych, D., Olszewski, M. B., Gutkowska, M., Helwak, A., Zyllicz, M., and Zyllicz, A. (2009) Hsp70 molecular chaperones are required to support p53 tumor suppressor activity under stress conditions. *Oncogene* **28**, 4284–4294
 27. Sharma, A. K., Ali, A., Gogna, R., Singh, A. K., and Pati, U. (2009) p53 amino terminus region (1–125) stabilizes and restores heat denatured p53 wild phenotype. *PLoS One* **4**, e7159
 28. Lavrarr, J. L., and Farnham, P. J. (2004) Use of transient chromatin immunoprecipitation assays to test models for E2F1-specific transcriptional activation. *J. Biol. Chem.* **279**, 46343–46349
 29. Somers, K. D., Merrick, M. A., Lopez, M. E., Incognito, L. S., Schechter, G. L., and Casey, G. (1992) Frequent p53 mutations in head and neck cancer. *Cancer Res.* **52**, 5997–6000
 30. Chandrachud, U., and Gal, S. (2009) Three assays show differences in binding of wild-type and mutant p53 to unique gene sequences. *Technol. Cancer Res. Treat.* **8**, 445–453
 31. Bajgelman, M. C., and Strauss, B. E. (2006) The DU145 human prostate carcinoma cell line harbors a temperature-sensitive allele of p53. *Prostate* **66**, 1455–1462
 32. Goh, A. M., Coffill, C. R., and Lane, D. P. (2011) The role of mutant p53 in human cancer. *J. Pathol.* **223**, 116–126
 33. Joerger, A. C., and Fersht, A. R. (2008) Structural biology of the tumor suppressor p53. *Annu. Rev. Biochem.* **77**, 557–582
 34. Shangary, S., and Wang, S. (2009) Small-molecule inhibitors of the MDM2-p53 protein-protein interaction to reactivate p53 function: a novel approach for cancer therapy. *Annu. Rev. Pharmacol. Toxicol.* **49**, 223–241
 35. Wiman, K. G. (2010) Pharmacological reactivation of mutant p53: from protein structure to the cancer patient. *Oncogene* **29**, 4245–4252
 36. Kim, H., Kim, K., Choi, J., Heo, K., Baek, H. J., Roeder, R. G., and An, W. (2011) p53 requires an intact C-terminal domain for DNA binding and transactivation. *J. Mol. Biol.* [10.1016/j.jmb.2011.12.001](https://doi.org/10.1016/j.jmb.2011.12.001)